JOURNAL OF QUATERNARY SCIENCE (2023) 38(3) 295–307 ISSN 0267-8179. DOI: 10.1002/jqs.3489

JQS Journal of Quaternary Science QRA Quaternary Research Association

Orbital- to millennial-scale variation of the speleothem $\delta^{18}O$ record during Marine Isotope Stages 5 to 3 on the southeast Chinese Loess Plateau and its climatic and environmental implications

YANJUN CAI,[1,2,3]* HAI CHENG,[1] XING CHENG,[2] ZHENGGUO SHI,[2] YANBIN LU,[2] LE MA,[2] CARLOS PÉREZ-MEJÍAS,[1] HAIWEI ZHANG,[1] YINGYING WEI,[2] GANG XUE,[4] HANYING LI,[1] MEI HE,[2] TING WANG,[1] R. LAWRENCE EDWARDS[5] and ZHISHENG AN[2]

[1]Institute of Global Environmental Change, Xi'an Jiaotong University, Xi'an, China
[2]State Key Laboratory of Loess and Quaternary Geology, Institute of Earth Environment, Chinese Academy of Science, Xi'an, China
[3]Open Studio for OCCEC, Qingdao National Laboratory for Marine Science and Technology, Qingdao, China
[4]State Key Laboratory of Continental Dynamics, Department of Geology, Northwest University, Xi'an, China
[5]Department of Earth Sciences, University of Minnesota, Minneapolis, Minnesota, USA

Received 3 June 2022; Revised 7 October 2022; Accepted 18 November 2022

ABSTRACT: The Chinese Loess Plateau (CLP) is located in northern China, a region climatically dominated by the East Asian monsoon. Speleothem records from this region are crucial to fully understand the variability of the East Asian summer monsoon (EASM) and reconcile the disparity seen between loess records and speleothem $\delta^{18}O$ records for the EASM. Here, we present an absolutely dated stalagmite isotope record spanning most of Marine Isotope Stage (MIS) 5 to MIS 3 from Xiaotian Cave, southeast CLP. The Xiaotian speleothem $\delta^{18}O$ record is dominated by precessional variations and punctuated by notable millennial-scale oscillations; in particular, the $\delta^{18}O$ values in MIS 5e, 5c and 5a were in the same range, consistent with other speleothem $\delta^{18}O$ records from the EASM region within quoted errors, verifying the difference between speleothem $\delta^{18}O$ and loess records (e.g. magnetic susceptibility) and the proposition that those two archives may record different aspects of the EASM changes. The similar values in MIS 5e, 5c and 5a observed from the speleothem $\delta^{18}O$ records in EASM regions, incompatible with the relatively higher North Hemisphere Summer Insolation (NHSI) during MIS 5e, were probably caused by an equivalent or even increased contribution of ^{18}O-enriched moisture from the South China Sea and North Pacific, implying that an El Niño-like state existed during MIS 5e. The Xiaotian $\delta^{18}O$ values increased abruptly at ~121.7 thousand years (kyr) before the present (BP, present refers to AD 1950), consistent with the trend seen in previously reported Chinese speleothem $\delta^{18}O$ records, indicating an abrupt regime shift in atmospheric circulations or hydroclimate conditions in the Asian monsoon systems. It cannot be definitely ruled out that an increase in sea ice extent in the northern North Atlantic, responding to a decrease of NHSI, reached a threshold to have led to abrupt changes in the Asian summer monsoon (ASM) through rapid shifts in the position of circulation of the westerlies and/or in the position of Intertropical Convergence Zone (ITCZ). Here, we hypothesized that sea surface cooling in the tropical Indian and Pacific Ocean caused by the decreased summer insolation reached a threshold that eventually resulted in an abrupt shift to more positive precipitation $\delta^{18}O$, either through weakened convection over the tropical ocean, or through abrupt shifts in moisture transport and cycling of tropical moisture sources for the ASM. The Xiaotian speleothem $\delta^{18}O$ record also shows centennial-scale variability with amplitude up to 3‰ within MIS 5e. These changes are similar to variations recorded by the speleothem $\delta^{18}O$ record from Tianmen Cave on the south-central Tibetan Plateau and Shangxiaofeng Cave in Shandong Province, northern China, suggesting a heightened sensitivity of precipitation $\delta^{18}O$ to climate changes at the marginal zone of the ASM even during the warm and humid MIS 5e interglacial. Climatic oscillations during MIS 5e appear to be comparable to those typical of the Holocene, implying rather unstable climate conditions during the Last Interglacial. © 2022 John Wiley & Sons, Ltd.

KEYWORDS: abrupt changes; Chinese Loess Plateau; Last Interglacial; stable isotopes; stalagmite

Introduction

Speleothems and loess records are among two of the most important archives in China for studying and understanding past changes in the Asian monsoon. However, some disparities are found when proxy records from both archives are compared. Chinese speleothem $\delta^{18}O$ records from southern China reveal strong periodicity in the precession (ca 23 kyr) band over the last 640 kyr (Cheng *et al.*, 2016), while the loess records (e.g. magnetic susceptibility) from northern China exhibit dominant glacial–interglacial (~100 kyr) cycles after the Middle Pleistocene Transition (Sun *et al.*, 2006). This disparity has been hotly debated in the paleoclimate community (Cheng *et al.*, 2021, and references therein) for the East Asian summer monsoon (EASM), since both loess and speleothems have been regarded as the main representative archives of EASM changes. In that regard, various interpretations have been proposed to reconcile the above-mentioned discrepancies.

From the perspective of loess records, classic EASM proxies (i.e. susceptibility and chemical weathering index) show a distinct signal of glacial–interglacial cycles (An *et al.*, 1991; Chen *et al.*, 1999a). Until recently, precessional and obliquity

*Correspondence: Yanjun Cai, as above
Email: yanjun_cai@xjtu.edu.cn

periodicities have been identified from other newly extracted proxies from Chinese loess deposits. For instance, the $\delta^{13}C$ records of loess show coexistence of 100-, 41- and 23-kyr periodicities (Sun *et al.*, 2015); the ^{10}Be-reconstructed monsoon precipitation variations were dominated by both precessional and glacial–interglacial (~100 kyr) periodicities over the last 550 kyr (Beck *et al.*, 2018); and the microcodium Sr/Ca records show dominant obliquity cycles (41-kyr) (Li *et al.*, 2017). These varied dominant periodicities among loess proxies have been ascribed to different effects, including the contrasted dependence of periodicity on varied proxies, the interference of sedimentary rate of loess deposits, and a potential insensitivity of some records to changes in precipitation on the Chinese Loess Plateau (CLP) (Sun *et al.*, 2015, Sun *et al.*, 2019; Cheng *et al.*, 2021). Specifically, low sedimentation rates and strong post-depositional pedogenic processes during interglacials usually attenuate the precessional signal in loess sequences from the central CLP (Feng *et al.*, 2004; Ma *et al.*, 2017), whereas magnetic susceptibility is sensitive to both temperature and precipitation changes, and might be somehow negatively correlated with precipitation if rainfall amount exceeds 1100 mm per year (Lv *et al.*, 1994).

From the perspective of speleothem $\delta^{18}O$ records, Cheng *et al.* (2012) proposed a threshold hypothesis which suggests that the amount-weighted annual precipitation $\delta^{18}O$ may be virtually determined by the summer precipitation $\delta^{18}O$ once summer monsoon precipitation amount surpasses a certain threshold, hindering further depletion of annual precipitation $\delta^{18}O$ during interglacial periods, and thus eventually muting the glacial–interglacial variance. Comparing speleothem records from southwest China controlled by the Indian summer monsoon (ISM), with those from southern China, mainly controlled by the EASM, and corroborated by model simulations, Cai *et al.* (2015) proposed that a muted glacial–interglacial signal in speleothem $\delta^{18}O$ records from southern China is possibly induced by changes in rainout processes, atmospheric circulation and moisture trajectories. In particular, these effects may be amplified by the large-scale glacial exposure of the western Pacific continental shelf and the 'land bridge' with maritime continents in the western equatorial Pacific. Recently, Liu *et al.* (2020a) argued that an increased temperature gradient and suppressed plant transpiration may enhance progressive rainout of Asian summer monsoon (ASM) moisture during glacials, resulting in a muted glacial–interglacial signal in Chinese speleothem $\delta^{18}O$ records. Additionally, the link between the different geographical locations of the records and its periodicity signal has coped with the observation of weak or even muted glacial–interglacial signals in the speleothem $\delta^{18}O$ records from southern China, and loess records come mainly from northern China. Thus, the different sensitivity between high- and low-latitude climates within China may also contribute to such contrasted signals between the two paleoclimate archives (Sun *et al.*, 2015). Comparing different archives from the same region may avoid the different sensitivity of high- and low-latitude climates to varied forcings (e.g. insolation and ice volume) and help to fully understand the climate and environment changes and their dynamics. Hence, more speleothem records from northern China are needed to further understand the cited different signals between speleothem and loess records, in line with recent studies (Li *et al.*, 2020).

Here, we present a precisely dated speleothem oxygen and carbon isotope record from the southeast CLP in northern China, to infer past precipitation $\delta^{18}O$ at the study site spanning much of the period from 130 to 50 kyr BP. Our study aims to characterize the variability in precipitation $\delta^{18}O$ at the CLP in northern China, to be able to compare speleothem $\delta^{18}O$ records for the EASM from North China with those from South China, and thus to investigate the potential factors contributing to the contrasted signal seen between speleothem $\delta^{18}O$ and loess deposits, and eventually to further understand the dynamics behind the EASM and possible heterogeneities. Related millennial- to centennial-scale variations of the EASM during Marine Isotope Stage (MIS) 5e and the abrupt shift of precipitation $\delta^{18}O$ during the MIS 5e–5d transition are also discussed.

Geographical setting, samples and analytical methods

Study cave

Xiaotian cave (35.47°N, 112.03°E, 1456 m above sea level, masl), is located in Qinshui County, Shanxi Province, northern China, southwest CLP (Figure 1). Mean temperature within the cave is ~12°C. It is close to the mean annual surface temperature (12.6°C) measured at Qinshui County meteorological station (35.68°N, 112.18°E, 875 masl) over the period 1961–2010. Mean annual precipitation is about 484 mm and more than 70% occurs in summer (June–September). The cave was formed in the Ordovician Majiagou Group limestone. It spans about 300 m length separated into two chambers by a narrow passage, resulting in poor ventilation and high relative humidity (close to 100%) inside the inner chamber where the stalagmite samples were collected in 2012.

Local climate

Xiaotian Cave is located in the southeast part of the CLP, a region close to the EASM front where limited precipitation (~200–400 mm) engenders the formation of a transition zone (also regarded as a marginal zone of the EASM) from a semi-humid to semi-arid/arid climate (Figure 1). Both meteorological observations and model simulations (Ding *et al.*, 2007; Liu *et al.*, 2014) indicate that regional precipitation in this region is sensitive to EASM changes, making use of the speleothem records from this region of interest. In particular, the pronounced precipitation seasonality (i.e. frequent heavy rains during the summer half year, and lower precipitation during the winter half year) results in a clear control of summer monsoon precipitation in the epikarst groundwater recharge, and thus conditioning drip water discharge within the cave. Conversely, the scarce rainfall of the winter dry season appear not to be effective in recharging the groundwater in the context of very dry surface soil. Given that a temperature effect dominates in winter while an amount effect dominates in summer in this area (Johnson and Ingram, 2004), winter precipitation barely recharges the vadose zone in this semi-arid region and thus it has minor influence on cave drip water, which is mainly supplied by summer monsoon precipitation. In that way, it may well capture changes in precipitation during the wet season (i.e. summer monsoon intensity), similar to the pattern seen in other caves from semi-arid areas, even if the wet season is not during summer (Pérez-Mejías *et al.*, 2018). In addition, the relatively low humidity in this semi-humid/semi-arid region may potentially increase evaporation of raindrops under cloud cover (Lee *et al.*, 2012; Pérez-Mejías *et al.*, 2018). This process may amplify the signal of precipitation $\delta^{18}O$ in a context of dryness, as a weak monsoon and less precipitation are generally associated with a reduced rainout through the moisture pathway to the study site, resulting in an increased precipitation $\delta^{18}O$ (Liu *et al.*, 2014).

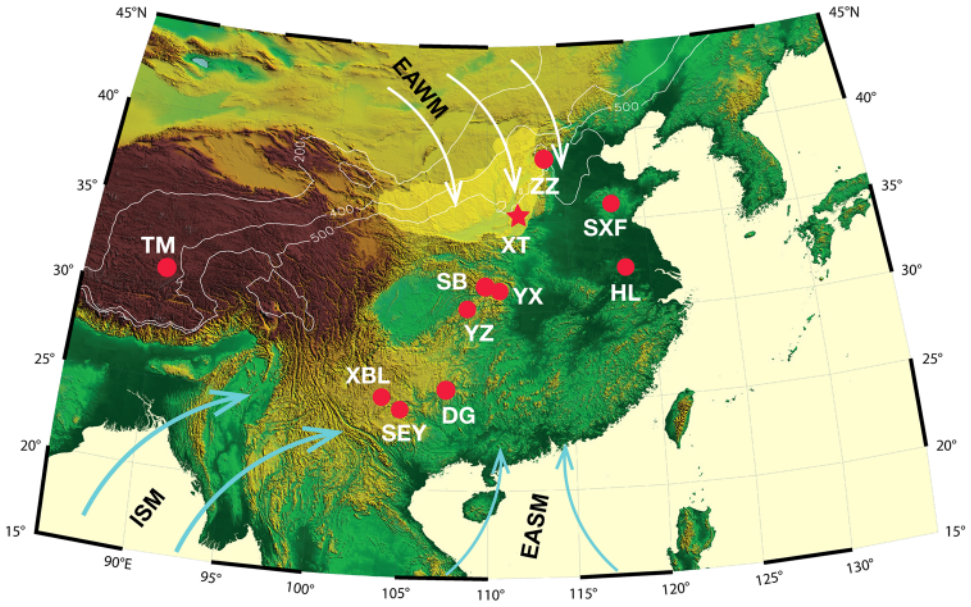

Figure 1. Topography of the study area, including the studied cave (red star) and other caves (red circles) mentioned in the text. The light blue arrows illustrate both summer monsoons (East Asian and Indian summer monsoons). The white arrows indicate the East Asian winter monsoon. The thin white lines represent annual precipitation isolines of 200, 400 and 500 mm. The yellow-shaded region indicates the Chinese Loess Plateau. The acronyms used to identify cave names are: XT, Xiaotian Cave (this study); TM, Tianmen Cave (Cai *et al.*, 2010a); XBL, Xiaobailong Cave (Cai *et al.*, 2015); SEY, unnamed Cave in southeast Yunnan (Liu *et al.*, 2020a); DG, Dongge Cave (Kelly *et al.*, 2006; Yuan *et al.*, 2004); YZ, Yangzi Cave (Wu *et al.*, 2020); SB, Sanbao Cave, (Wang *et al.*, 2008; Cheng *et al.*, 2009); YX, Yongxing Cave (Chen *et al.*, 2016); HL, Hulu Cave (Wang *et al.*, 2001); SXF, Shangxiaofeng Cave (Xue *et al.*, 2019); ZZ, Zhenzhu Cave (Li *et al.*, 2020). [Color figure can be viewed at wileyonlinelibrary.com]

As a whole, the amount of precipitation and the oxygen isotope composition are susceptible to EASM changes.

Stalagmite sample and analytical methods

Two stalagmites (XT-4 and XT-5) were used for this study, both collected from the inner chamber, ~270 m from the cave entrance. XT-4 is ~9.5 cm long and ~5.5 cm in diameter, while XT-5 is ~16.2 cm long and ~6.0 cm in diameter. We cut the stalagmites using a diamond wire saw, and the halves were polished (Figure 2). Sub-samples for ^{230}Th dating were drilled along the growth layers at various depths and always following the growth axes, using a handheld carbide dental drill with a 0.9-mm drill bit. The drilled powder, about 100 mg per sample, was dated at the Isotope Laboratory, Xi'an Jiaotong University, using multi-collector inductively coupled plasma mass spectrometry (MC-ICP-MS). The chemical protocols used to separate uranium and thorium for ^{230}Th dating are adapted from those described in Edwards *et al.* (1987), and the instrumental analysis procedures are detailed in Cheng *et al.* (2013). The initial atomic ratio of $4.4 \pm 2.2 \times 10^{-6}$ of $^{230}Th/^{232}Th$ was used for correcting the initial ^{230}Th contamination. As indicated by the low ^{232}Th concentration, the initial ^{230}Th in most dating samples seems to be insignificant and the corrections are well within analytical uncertainties, except for two subsamples with relatively high detritus contamination (Table S1). Within quoted errors, all the dates are in stratigraphic order.

Subsamples for stable isotope measurement were collected at intervals of 0.15–0.20 mm for XT-4 by using micromill, and at intervals of 0.5 mm for XT-5 by using a handheld dental drill with 0.3-mm drill bits. All the subsamples were analysed in an Isoprime100 gas source stable isotope ratio mass spectrometer equipped with a MultiPrep system at the Institute of Earth Environment, Chinese Academy of Sciences. The inter-laboratory standard TB1 was run for every 10 samples and arbitrarily selected duplicate measurements were taken every 10 to 20 samples, respectively, to check reproducibility. $\delta^{18}O$ and $\delta^{13}C$ values are reported in the δ notation, the per mil deviation with reference to the Vienna PeeDee Belemnite (VPDB) standard ($\delta^{18}O=[((^{18}O/^{16}O)_{sample}/(^{18}O/^{16}O)_{standard} - 1) \times 1000]$). Precision in the $\delta^{18}O$ and $\delta^{13}C$ measurements is better than 0.15 and 0.12‰ (2σ), respectively.

Results

Chronology

Eighteen ^{230}Th dates attained from XT-4 indicate that it grew at 130–121 kyr BP, with a hiatus between ~123 and 126 kyr BP (Figure 2). Likewise, another 18 ^{230}Th dates from XT-5 show that the stalagmite was deposited from ~86.8 to 13.3 kyr BP, with two hiatuses seen between ~71.2–61.7 and ~49.3–16.1 kyr BP (Figure 2). In this study, we omitted the top portion of XT-5 due to its short duration and the switch to stalactite in that part. The COPRA package for Matlab (Breitenbach *et al.*, 2012) was used to establish the final chronology (depth–age models) for each stalagmite (Figure 3). Due to the hiatuses found in the samples, we apply this approach to the two segments of continuous growth in each stalagmite, respectively. We also explored an additional model based on linear interpolation to check the difference between these two approaches. The comparison shows that the age differences between these two methods are relatively small, typically less than 275 and 40 years for stalagmites XT-4 and XT-5, respectively.

Speleothem $\delta^{18}O$ and $\delta^{13}C$ records

The sampling strategies (i.e. micromilling and drilling on the polished surface) produced a temporal resolution of the speleothem $\delta^{18}O$ and $\delta^{13}C$ records ranging from ~3 to ~54 years for XT-4, and from ~8 to 180 years for XT-5, respectively. The speleothem $\delta^{18}O$ values vary between −12.3 and −7.2‰, with a maximum range of ~5.1‰ (Figure 4). The speleothem $\delta^{13}C$ values fluctuate between −12.5 and −3.4‰, with a maximum range of ~9.1‰. The most prominent feature

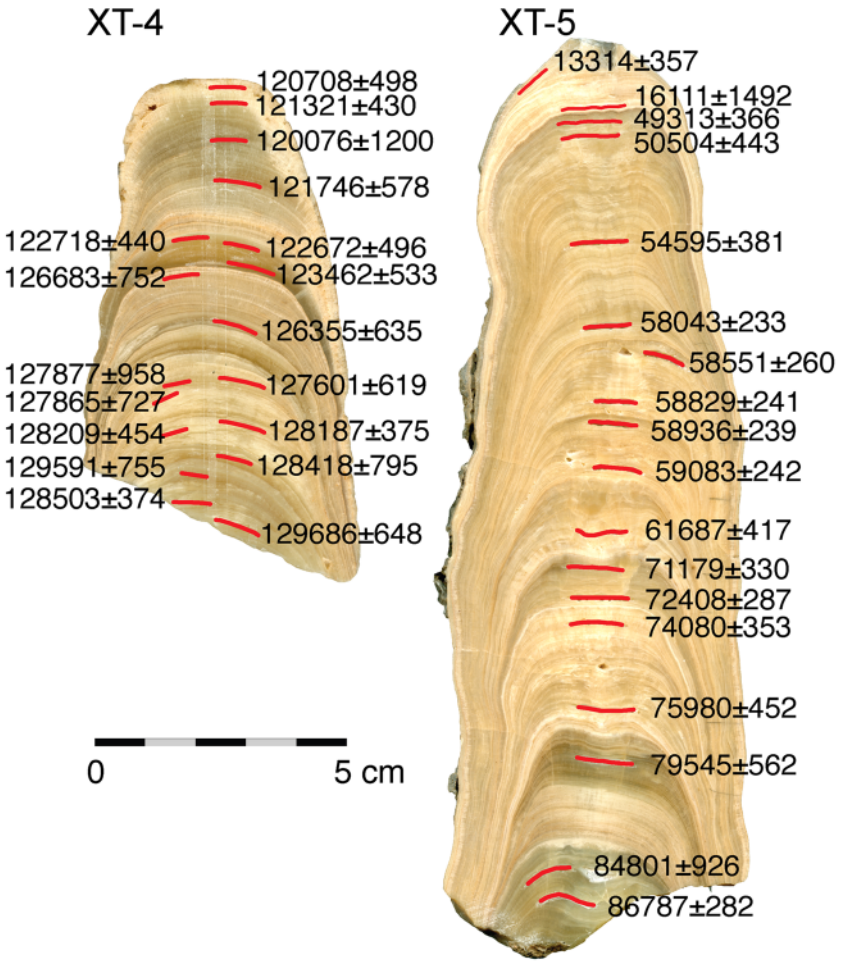

Figure 2. Polished sections of stalagmites XT-4 and XT-5 from Xiaotian Cave. U-series dates are also presented beside the drilling positions. [Color figure can be viewed at wileyonlinelibrary.com]

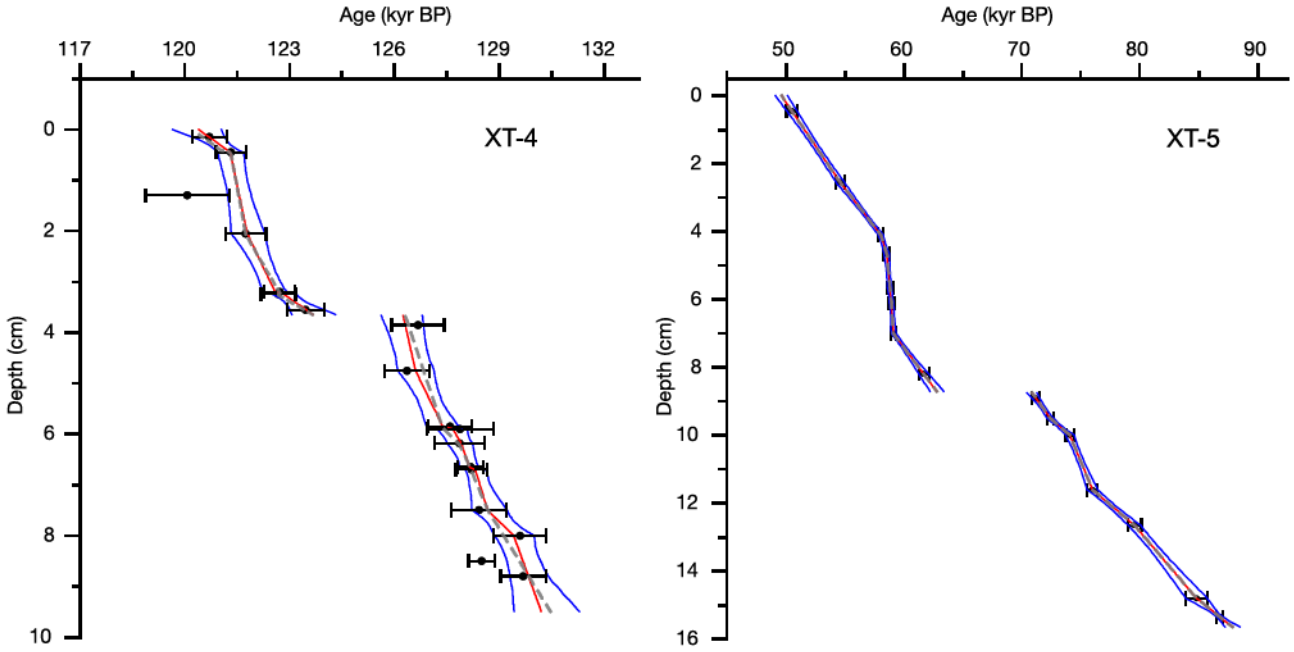

Figure 3. Age versus depth plots for stalagmites XT-4 and XT-5. All ages of the stalagmites are presented as thousand years before present (1950), kyr BP. Error bars indicated in the plots are 2σ errors. The COPRA package for Matlab (Breitenbach *et al.*, 2012) was used to establish the chronologies of these two stalagmites. The blue line indicates the 95% confidence level, while the red line shows the chronologies used for the stable isotope time series. The dashed grey line indicates the linear interpolated chronologies. [Color figure can be viewed at wileyonlinelibrary.com]

exhibited in the speleothem $\delta^{18}O$ and $\delta^{13}C$ records is the large amplitude in the long term, suggesting a heightened sensitivity of the isotope composition of the present samples, notable in the speleothem $\delta^{13}C$, to abrupt climate changes. The speleothem $\delta^{18}O$ in our record shows similar variations to the well-studied cave records from Hulu, Sanbao and Yongxing caves, as well as the adjacent Zhenzhu Cave (Figure 5), within chronological uncertainties. Such similarities

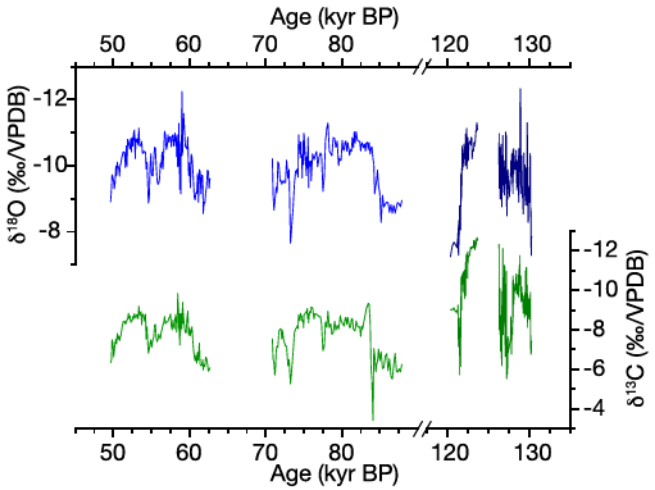

Figure 4. $\delta^{18}O$ (blue) and $\delta^{13}C$ (green) time series obtained from stalagmites XT-4 (dark colour) and XT-5 (light colour). [Color figure can be viewed at wileyonlinelibrary.com]

enable the replication of speleothem records from different caves and provide further evidence of the climatic relevance of the present record. It indicates that stalagmites XT-4 and XT-5 appear to have been deposited in near-equilibrium conditions with cave drip water, and thus the stalagmite $\delta^{18}O$ appears to have been controlled by the $\delta^{18}O$ of the drip water and the cave temperature (Hendy, 1971, Dorale, *et al.*, 1998; Wang *et al.*, 2001).

Discussion

The interpretation of $\delta^{18}O$ and $\delta^{13}C$

The interpretation of speleothem $\delta^{18}O$

Replication of the Xiaotian speleothem $\delta^{18}O$ record and other speleothem $\delta^{18}O$ records from southern China suggests that the stalagmites in this study were formed under (or near) isotope equilibrium conditions, and so the stable isotopes may reflect climate conditions. In that regard, the speleothem $\delta^{18}O$ may have been dominated by the isotope composition of drip water (i.e. amount-weighted mean of the precipitation $\delta^{18}O$) and temperature (Hendy, 1971). The large amplitude of the speleothem $\delta^{18}O$ record (i.e. 5.1‰) is unlikely to be interpreted as temperature changes within the cave, since the temperature-dependent fractionation between calcite and drip water is about −0.23‰ °C^{-1} (Kim and O'Neil, 1997). Therefore, the changes in the speleothem $\delta^{18}O$ were probably largely dominated by drip water $\delta^{18}O$, although we cannot completely rule out an influence of the temperature effect.

As summer precipitation in this region accounts for up to 70% of annual precipitation, and winter precipitation is unlikely to effectively infiltrate through the epikarst, the changes in summer precipitation $\delta^{18}O$ are expected to be the primary factor influencing speleothem $\delta^{18}O$. In regions affected by the EASM, multiple factors or processes have been suggested to explain the variations in precipitation $\delta^{18}O$, as summarized in Cai *et al.* (2021), despite the debates on the interpretation of speleothem $\delta^{18}O$ in East Asian monsoon regions (Liu *et al.*, 2020b, and references therein). These factors include the changing ratio of summer versus winter (or autumn–winter) precipitation (Wang *et al.*, 2001, Rao *et al.*, 2015), the rainout process of the air mass as it moves over the continent (Yuan *et al.*, 2004; Cheng *et al.*, 2009), the amount of precipitation at the study region and changes in the moisture sources (Cai *et al.*, 2001; 2015; Maher, 2008; Tan, 2014). Since the epikarst is mainly charged by summer precipitation in this semi-arid region, it is therefore reasonable to exclude the influence of a change in the ratio of summer/winter precipitation. Here, the interpretation of speleothem $\delta^{18}O$ is in line with that of the rainout history of moisture transported to the cave; that is, lower $\delta^{18}O$ values generally indicate more distal moisture source(s) in tandem with enhanced *en route* rainout linked to a stronger summer monsoon and vice versa (Cai *et al.*, 2021, Cheng *et al.*, 2016). At the same time, we acknowledge that changes in atmospheric circulation and moisture sources, as well as moisture recycling (Cai *et al.*, 2001; 2015; Maher, 2008; Tan, 2014) may contribute significantly to precipitation $\delta^{18}O$ in our study region. We discuss some of these influences below.

The interpretation of speleothem $\delta^{13}C$

Speleothem $\delta^{13}C$ has often been linked to various factors, including the type of vegetation (i.e. C_3 vs C_4) above the cave, which determine the $\delta^{13}C$ of soil CO_2, biomass, which affects the soil CO_2 concentration, biological activities in the soil, carbon component dissolved from the host rock and prior carbonate precipitation (PCP) in the epikarst and within the cave (McDermott, 2004; Genty *et al.*, 2006; Ridley *et al.*, 2015; Lechleitner *et al.*, 2017; Fohlmeister *et al.*, 2020; Xue *et al.*, 2021). In northern China, precipitation is the dominant factor affecting vegetation density and/or types and then plays an important role in causing changes in the speleothem $\delta^{13}C$ record (Li *et al.*, 2020). In the present record, the speleothem $\delta^{13}C$ variations resemble that of $\delta^{18}O$ on orbital to millennial timescales in terms of timing and structure (Figure 4), indicating both speleothem $\delta^{13}C$ and $\delta^{18}O$ were affected by common forcings on these timescales, probably reflecting changes in local effective rainfall associated with intensity of the EASM. Such a correlation is in line with an interpretation of low $\delta^{13}C$ values pointing to intensified EASM rainfall, enhanced soil CO_2 production and reduced PCP in the epikarst above the cave, whereas high values result from reduced microbial activity in the soil and enhanced PCP under drier conditions (Li *et al.*, 2020). Furthermore, the Sr/Ca ratios of these two stalagmites show similar variations to speleothem $\delta^{13}C$ and $\delta^{18}O$ records while Mg/Ca ratios display changes at odd or even anti-correlated with those three records (Supporting Information Fig. S1), implying that vegetation and soil dynamics probably play an important role in controlling millennial- to orbital-scale variations in speleothem $\delta^{13}C$, supported by its correlation with Sr/Ca. The variable or even anti-correlated relationships between Mg/Ca ratios and stable isotope ratios suggest that multiple sources of magnesium in this area may hamper its use as a hydrological proxy.

Orbital- to millennial-scale variation of speleothem $\delta^{18}O$ and the comparison with other records

Based on the present Xiaotian speleothem $\delta^{18}O$ and $\delta^{13}C$ record, we are able to infer the EASM variability on orbital to millennial timescales. On an orbital timescale, the sinusoidal-peak-like variations of stalagmite $\delta^{18}O$ during periods from 130 to 120 kyr BP, from 85 to 72 kyr BP and from 60 to 50 kyr BP are essentially in agreement with the timing seen in the North Hemisphere Summer Insolation (NHSI), further confirming the direct link between the ASM and NHSI (Kutzbach *et al.*, 1981; Wang *et al.*, 2008; Cheng *et al.*, 2009, 2016; Shi *et al.*, 2011). The consistency between speleothem $\delta^{18}O$ records from the CLP (i.e. Xiaotian and Zhenzhu Caves) and other speleothem $\delta^{18}O$ records from South China demonstrates that the difference between speleothem $\delta^{18}O$ and loess records (e.g. magnetic

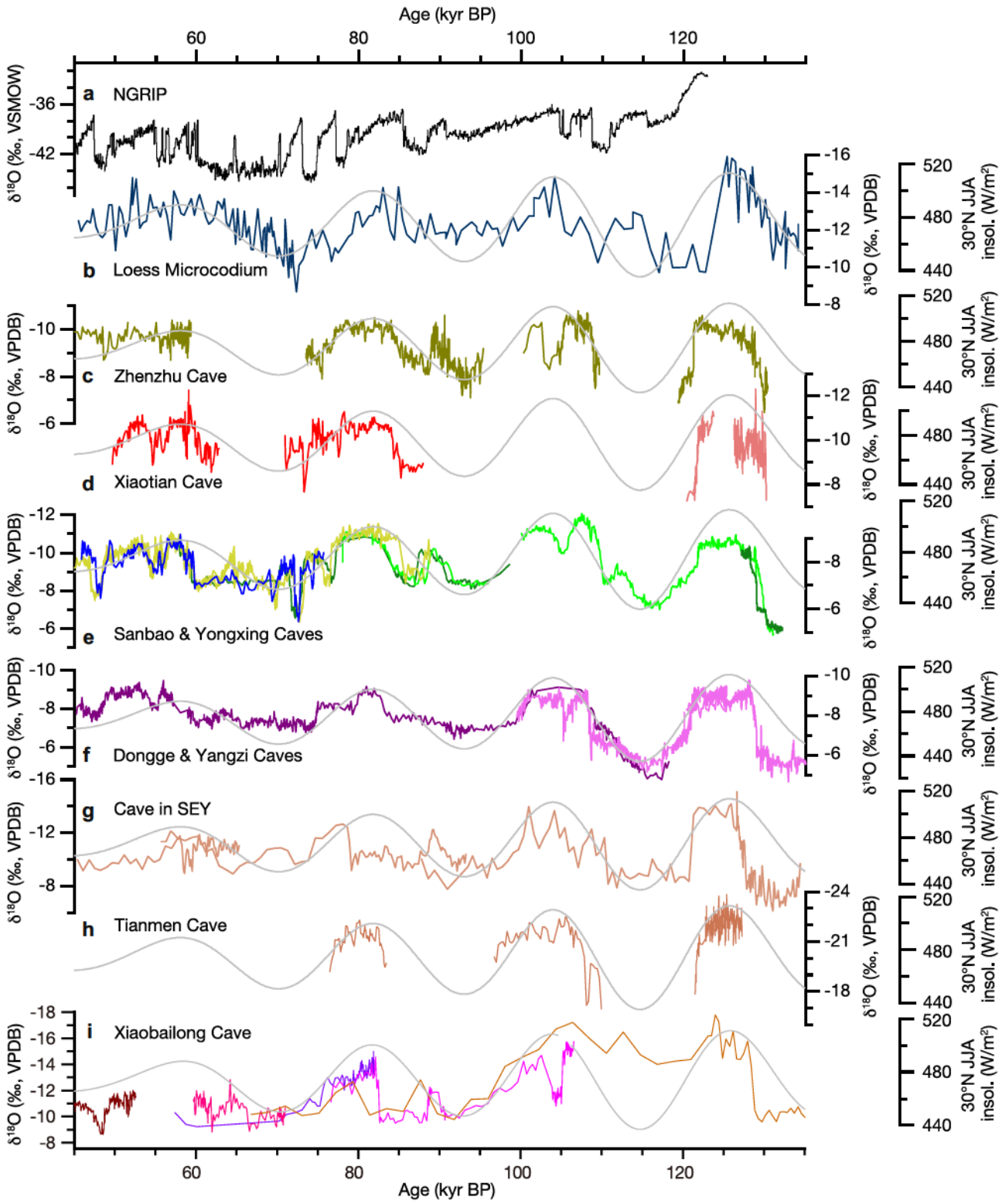

Figure 5. Comparison of oxygen isotopic records from Xiaotian Cave (d, stalagmites XT-4 and XT-5) with microcodium $\delta^{18}O$ records from loess deposits (b, Zhang *et al.*, 2021), $\delta^{18}O$ records from Zhenzhu (c, Li *et al.*, 2020), Sanbao and Hulu (e, blue and green lines, Wang *et al.*, 2001; 2008), Yongxing (e, yellow-green line, Chen *et al.*, 2016), Dongge (f, pink line, Kelly *et al.*, 2006) and Yangzi caves (f, purple line, Wu *et al.*, 2020), an unnamed Cave from southeast Yunnan (g, Liu *et al.*,2020a), Tianmen Cave (h, Cai *et al.*, 2010a) and Xiaobailong Cave (i, Cai *et al.*, 2015), and $\delta^{18}O$ record of Greenland ice core (a, NGRIP Members, 2004). Grey lines show the Northern Hemisphere summer (JJA) insolation at 30°N. [Color figure can be viewed at wileyonlinelibrary.com]

susceptibility) can be ascribed to the fact that they record different aspects of the EASM changes (Cai *et al.*, 2010b; Cheng *et al.*, 2021), rather than a different signal to the ASM between regions. Moreover, the microcodium $\delta^{18}O$ record of loess deposits, which largely reflect summer precipitation $\delta^{18}O$, displays distinct precessional cycles, consistent with speleothem $\delta^{18}O$ records (Zhang *et al.*, 2021), further substantiating the coherent variation of precipitation $\delta^{18}O$ in regions affected by the EASM on orbital timescales.

On millennial timescales, the abrupt shifts of speleothem $\delta^{18}O$ (e.g. 56 kyr BP) align very well with the Greenland ice core $\delta^{18}O$ changes (Figure 5; NGRIP Members, 2004). In particular, there are double peaks of high $\delta^{18}O$ in the Greenland ice core record at GIS 15 that are also apparent

in our speleothem $\delta^{18}O$ record, indicating the close dynamic connection between climate at high northern latitudes and the EASM (Wang *et al.*, 2001), probably through the westerlies (Porter and An, 1995; Chiang *et al.*, 2015). However, the iconic saw-tooth patterns of the GIS events in ice core $\delta^{18}O$ records (i.e. an abrupt increase and a more gradual decrease) are not manifested in our speleothem $\delta^{18}O$ record nor in nearby speleothem $\delta^{18}O$ records from Zhenzhu Cave (Li *et al.*, 2020). Similar to other speleothem $\delta^{18}O$ records from Hulu (Wang *et al.*, 2001), Sanbao (Wang *et al.*, 2008) and Yongxing (Chen *et al.*, 2016) caves in South China (Figure 5), our speleothem $\delta^{18}O$ display a trapezoidal-like pattern, that is a decrease at the beginning and increase at the end with similar rate and oscillating around a mean value in between. This observation suggests a coupled forcing which may operate among high-latitude temperatures, tropical moisture transport and the potential impacts from the Southern Hemisphere through trans-equatorial flows (Cai *et al.*, 2006; Rohling *et al.*, 2009; Cheng *et al.*, 2021), and so a single forcing factor cannot fully account for the EASM variations on millennial timescales.

The speleothem $\delta^{13}C$ profile features systematically lower $\delta^{13}C$ values during MIS 5e and relatively higher $\delta^{13}C$ values during MIS 5a and MIS 3, showing a contrasted pattern compared to the $\delta^{18}O$ values. This observation probably suggests a distinct climatic and environmental alteration responding to the ice-volume changes through vegetation and soil dynamics changes, caused by changes in either precipitation, temperature or both. However, we are conservative in interpreting this feature and the related inference, since the contrast between MIS 5e and 5a and 3 comes from two different stalagmites and might be caused by differences in cave infiltration systems for these two stalagmites.

Muted response of speleothem $\delta^{18}O$ to insolation during MIS 5e

The Xiaotian speleothem $\delta^{18}O$ record broadly replicates the speleothem $\delta^{18}O$ record from Zhenzhu Cave, although slight differences can be found around 77 kyr and from 55 to 50 kyr BP, probably caused by uncertainties in the chronology of the latter. The similarity of these two records supports the reliability of our record to infer precipitation $\delta^{18}O$ changes in northern China. Moreover, these two records also align well with other Chinese speleothem records from monsoon regions, i.e. Sanbao (Wang *et al.*, 2008), Yongxing (Chen *et al.*, 2016), Hulu (Wang *et al.*, 2001), Dongge (Kelly *et al.*, 2006), Yangzi (Wu *et al.*, 2020), an unnamed cave in southeast Yunnan (SEY, Liu *et al.*, 2020a) and Tianmen (Cai *et al.*, 2010a) caves, further confirming a coherent temporal variation of precipitation $\delta^{18}O$ in Asian monsoon regions (Wang *et al.*, 2008; Cai *et al.*, 2012, 2015; Cheng *et al.*, 2016), and also the strong link between precipitation $\delta^{18}O$ and insolation in mid-latitude areas (e.g. Cheng *et al.*, 2019; Pérez-Mejías *et al.*, 2019). However, differences are seen in terms of the amplitude of speleothem $\delta^{18}O$ during MIS 5a, 5c and 5e. In caves under the influence of the ISM (e.g. Xiaobailong, SEY and Tianmen), the speleothem $\delta^{18}O$ values during MIS 5e were lower than that during MIS 5c and 5a (Figure 5), in line with the changes in NHSI. On the other hand, in caves under the influence of the EASM (Dongge, Yangzi, Xiaotian and Zhenzhu), there are similar speleothem $\delta^{18}O$ values in MIS 5e, 5c and 5a (Figure 5), indicating a muted response of speleothem $\delta^{18}O$ to insolation during MIS 5e. This disparity suggests that different processes may be involved in the precipitation $\delta^{18}O$ in EASM and ISM regions.

Cheng *et al.* (2012) proposed the 'threshold mechanism' 2012 to interpret this disparity, and argued that the amount-weighted annual precipitation $\delta^{18}O$ is determined largely by the ratio of summer to winter precipitation, rather than the average rainfall value. In that line, any increase in summer rainfall above a certain threshold could result in similar annual precipitation $\delta^{18}O$ values to those associated merely with the summer monsoon component. However, speleothem records from the Indian Monsoon region, where the precipitation $\delta^{18}O$ is determined mainly by the summer monsoon precipitation $\delta^{18}O$, suggest that $\delta^{18}O$ coming from the summer monsoon precipitation would be persistently depleted in ^{18}O, along with an intensified summer monsoon and enhanced rainout effect (Cai *et al.*, 2015). It is therefore unlikely that the 'threshold mechanism' could explain this disparity in the EASM domain.

Both observation and model simulations have shown that the moisture transported to the regions affected by the ISM (e.g. southwest China and southern Tibetan Plateau) predominantly came from the Bay of Bengal, with the precipitation $\delta^{18}O$ dictated by the rainout fractionation of moisture from the ocean source to the cave site during both glacial and interglacial periods (Cai *et al.*, 2010a; Cai *et al.*, 2015; Liu *et al.*, 2020a). Changes in the temperature gradient may have impacts on the glacial–interglacial variation of precipitation $\delta^{18}O$ (Liu *et al.*, 2020a). However, its influence might be small in the case of MIS 5c and 5e, since both periods exhibit an interglacial climate and the sea level in MIS 5c was only 20–30 m lower than that of MIS 5e (Spratt and Lisiecki, 2016). For the EASM, the thermal contrast seen between the heated East Asian continent and South China Sea on the one hand, and northwestern Pacific on the other, lead to a complex atmospheric circulation in the EASM domain, involving multiple moisture sources for monsoon precipitation in East Asia (Ding and Chan, 2005). Three major moisture conveying paths have been identified from modern observations and model simulations, i.e. Arabian Sea across the southern Bay of Bengal (the Indian Ocean path), South China Sea and the tropical Pacific, and North Pacific (Cai *et al.*, 2015, and references therein).

Several studies have suggested that changes in the contribution of different moisture sources would have resulted in a certain variability of precipitation $\delta^{18}O$ in East Asia. For instance, Cai *et al.* (2001) hypothesized that the Holocene high-amplitude fluctuations seen in the stalagmite $\delta^{18}O$ at Qixing Cave (Guizhou Province, southwest China) might be caused by changes in the contribution of different moisture sources, i.e. South China Sea vs. Arabian Sea. In the same line, Maher (2008) suggested that decreased Indian monsoon-sourced moisture over China would have resulted in increasing proportions of moisture sourced from the EASM and led to domination of the ISM on speleothem $\delta^{18}O$ in southern China during the Holocene. Pausata *et al.* (2011) suggested that changes in the speleothem $\delta^{18}O$ associated with Heinrich events in East Asia were determined by the intensity of Indian monsoon precipitation, since the precipitation $\delta^{18}O$ in China was controlled largely by the moisture imported from the Indian monsoon region. Analysing the relationship between the observational records of amount-weighted annual mean $\delta^{18}O$ of precipitation ($\delta^{18}O_w$) and meteorological variables, Tan (2014) advocated that the speleothem $\delta^{18}O$ value reflects the different influence of the ISM and EASM, which is associated with the intensity of southeast trade winds, affecting the moisture contributions from the Indian Ocean and West Pacific Ocean and South China Sea. Combining the speleothem $\delta^{18}O$ record from Xiaobailong Cave in southwest China and model simulations, Cai *et al.* (2015) proposed that changes in atmospheric circulation and associated moisture

contribution from different sources were probably the major factors contributing to the muted difference seen between glacial and interglacial speleothem $\delta^{18}O$ in southern China. Taking all this into consideration, it is not implausible that similar speleothem $\delta^{18}O$ values in MIS 5e (or even heavier, as seen in the Sanbao record), 5c and 5a in the East Asian monsoon region were caused by an equivalent or even increased contribution of the moisture from the South China Sea and North Pacific, which is enriched in ^{18}O as compared with moisture from the Indian Ocean and Bay of Bengal.

Modern observations indicate a teleconnection between surface temperature in the tropical Pacific Ocean and East Asian monsoons (including both summer and winter monsoons) through the varied size and intensity of the lower tropospheric anticyclone located in the western North Pacific (Wang, *et al.*, 2000). In that regard, any increase of sea surface temperature (SST) in the eastern Pacific may give rise to an anomalous lower-tropospheric anticyclone located in the western North Pacific. This anomaly persists during spring and early summer, resulting in more moisture coming from North Pacific and South China Sea that is transported to East China along the west boundary of the western Pacific subtropical high. The increased moisture contribution from nearby North Pacific and South China Sea eventually led to precipitation enriched in ^{18}O, and hence may have substantial impacts on the variation of precipitation $\delta^{18}O$ in East Asia. A set of numerical experiments have also been carried out to examine the sensitivity of the EASM and ISM to changes in the astronomical parameters during the interglacial periods of MIS 5c and 5e (Shi *et al.*, 2018). It was found that moisture from the Pacific Ocean is increased remarkably due to an anomalous anticyclone over the northwestern Pacific, enhancing its relative contribution to the annual precipitation in East China and resulting in enriched precipitation $\delta^{18}O$ during MIS 5e (Shi *et al.*, 2018). This experiment provides direct support for the dynamic connection discussed above. Recently, the comparison of SST records in the Pacific Ocean over the last 350 kyr, from the West (warm pool) to the East (cold tongue), indicates that the zonal temperature gradient decreased and exhibited an El Niño-like state during interglacial periods (Supporting Information Figure S2, Liu *et al.*, 2020c), implying that this dynamic connection cannot be discarded.

Similar disparities can be identified during older periods such as MIS 7.3, 15.1, 15.3 and possibly 9.3, as can be extracted from the longest speleothem $\delta^{18}O$ record from southern China by Cheng *et al.* (2016). As all these disparities occurred largely during the high insolation period following the deglaciation, in which ice melting occurred much faster than during the last deglaciation (Spratt and Lisiki, 2016), it is likely that during these periods the swiftly increased summer insolation warmed the Earth surface and elevated substantially the water vapour concentration in the lower troposphere. The increase in lower-tropospheric water vapour weakens the mass exchange between the boundary layer and the troposphere, and eventually slows down the zonal atmosphere circulation over the tropical Pacific Ocean (Held and Soden, 2006; Vecchi *et al.*, 2006), resulting in a decreased zonal temperature gradient similar to an El Niño-like state. Regardless, further model simulations are needed to confirm this hypothesis.

The abrupt shift of precipitation $\delta^{18}O$ from MIS 5e to MIS 5d

The Xiaotian speleothem $\delta^{18}O$ increased abruptly from −10.5 to −7.8‰ at 121.7 kyr BP, showing a pattern consistent with previously reported speleothem $\delta^{18}O$ records from Dongge, Sanbao and Tianmen caves during this period, and demonstrating that an abrupt change in precipitation $\delta^{18}O$ occurred within Asian monsoon regions at the end of MIS 5e. This abrupt increase in speleothem $\delta^{18}O$ largely follows the NHSI decrease, confirming the forcing of NHSI on the ASM (Kutzbach *et al.*, 1981; Wang *et al.*, 2008; Cai *et al.*, 2010a; Shi *et al.*, 2011; Cheng *et al.*, 2016). However, as recorded in various caves in South and East Asia, speleothem $\delta^{18}O$ persistently increased more than ~2‰ (even reaching higher values at Tianmen Cave, due to its high altitude) within less than ~500 years, probably indicating a regime shift in the atmospheric circulation, with clear repercutions for the hydroclimate conditions in the Asian monsoon domain.

Cheng *et al.* (2012) suggested that such a shift between two regimes was possibly related to abrupt climate events at high northern latitudes (Cheng *et al.* 2009; Ziegler *et al.* 2010) and/or due to some threshold mechanisms, such as the atmospheric humidity level over the oceans around the monsoon regions and its related feedbacks (Levermann *et al.* 2009; Schewe *et al.* 2011). A set of transient simulations of isotope-enabled climate models have been carried out to understand this abrupt change (Battisti *et al.*, 2014). However, no such abrupt shift has been identified in both precipitation and precipitation $\delta^{18}O$ in Asian monsoon regions, similar to the results in a previous modelling study by Kutzbach *et al.* (2008). It was then assumed that either slow changes in the mean state of the global ocean, caused by insolation forcing, led to abrupt changes in the sea ice extent in the North Atlantic, thereby changing abruptly the $\delta^{18}O$ of the sea and therefore of the rainfall throughout the Northern Hemisphere, or the threshold feedbacks in vegetation and/or soil properties to the smooth changes in climate cause abrupt changes in fractionation of soil water as it percolates to the cave (Battisti *et al.*, 2014). Since there was no proxy record of the ISM showing such abrupt changes, Battisti *et al.* (2014) rejected the hypothesis of abrupt sea-ice feedbacks. Soon after, multiple speleothem $\delta^{18}O$ records from the Indian monsoon region, which exhibit abrupt changes in line with those seen in speleothems from southern China, were reported (Cai *et al.*, 2015; Kathayat *et al.*, 2016), thus refuting Battisti *et al.*'s claims. Most recently, Yin *et al.* (2021) demonstrated that when the decreasing insolation reaches a certain threshold, an abrupt weakening of the Atlantic Meridional Overturning Circulation led to a cooler mean climate state, likely to occur at the end of each interglacial over the last 800 kyr. It is then possible that such abrupt shifts in the mean climate state in the North Atlantic cause abrupt changes in precipitation $\delta^{18}O$ in Asian monsoon regions by affecting the circulation of the westerlies and/or the Intertropical Convergence Zone (ITCZ). However, we noted that the marine sequences from the northern North Atlantic and terrestrial records from southern Europe did not indicate any distinct signal in the SST or in the Atlantic Meridional Ocean Circulation intensity during this period, although a series of multi-centennial intra-interglacial cold/arid oscillations have been stablished for the Last Interglacial (129–116 kyr BP) (Tzedakis *et al.*, 2018, and references therein). Also, the insolation threshold identified by Yin *et al.* (2021) occurs much later than the abrupt change in our speleothem $\delta^{18}O$ record. Whether this abrupt shift was forced by abrupt changes in the northern North Atlantic remains an open question.

The threshold feedbacks in vegetation and/or soil is another potential mechanism proposed to account for such an abrupt shift in speleothem $\delta^{18}O$ (Battisti *et al.*, 2014). However, the abrupt changes in speleothem $\delta^{18}O$ seen in records from different climatic zones, under a wide spectra of soil cover, minimize the chances of identifying the reason for the abrupt changes in a hypothetical ubiquitous change in the infiltration path of varied karst systems.

Recently, the study of a speleothem record from Guatemala (Central America) found that regional rainfall increased persistently within a 2000-year period and changed from a dry state to an active convective regime during the early Holocene, and suggested that this regime shift was driven by an increase in the SST exceeding a certain threshold in the nearby tropical ocean (Winter *et al.*, 2020). Although this diagnosis not relevant to the abrupt shift observed in our study, it suggests the possible existence of thresholds in the SST of the tropical Ocean, which may play an important role in the occurrence of an active convective regime. The latter has substantial impacts on the amount of precipitation as well as on the precipitation isotope composition. We hypothesize that the decline in insolation led to the SST decrease of the tropical Indian and Pacific Ocean, and once it reaches a certain threshold, a regime shift would occur in precipitation $\delta^{18}O$, either through the weakened convective atmospheric activity over the tropical ocean or through abrupt changes in moisture transport and cycling of tropical moisture sources of the ASM.

How stable was the Asian Monsoon during the Last Interglacial?

The Last Interglacial, also referred to as the Eemian, which lasted from 130,000 to 116,000 years ago (Kukla, 2000, and references therein), is one of the most important periods for palaeoclimate study, because it has similar orbital parameters to the present interglacial, i.e. the Holocene, and may provide an important reference scenario for understanding current global warming and to adapt to future climate change (Kukla *et al.*, 2002). How stable the climate was during the Last Interglacial has been hotly debated (Kukla, 2000; Tzedakis *et al.*, 2018). The first debate started with the large-amplitude oscillations seen in the GRIP ice core $\delta^{18}O$ during the Last Interglacial (Dansgaard *et al.*,1993; Greenland Ice-core Project, 1993), while the comparison of GISP2 and GRIP ice cores suggest that these oscillations were probably caused by an alteration of ice flow (Grootes *et al.*,1993; Taylor *et al.*,1993). Although some studies suggest that these large oscillations within the lower parts of ice cores may not be caused by stratigraphic disturbances (Johnsen *et al.*, 1995, 1997), detailed inspections and study of the NGRIP ice core argued that both GRIP and GISP2 ice cores were subject to stratigraphic disturbances in ice older than 110 ka BP, as evidenced by the bipolar data on atmospheric CH_4 and $\delta^{18}O$ of O_2 trapped in ice (Fuchs and Leuenberge, 1996; Chappellaz *et al.*, 1997). Meanwhile, various climate records from marine sediments indicated that there were substantial cold events or climatic oscillations during MIS 5e. For instance, the SST in the Northern Atlantic Ocean and Norwegian Sea decreased about 2 °C, and a moderate freshening of the North Atlantic occurred during the middle part of MIS 5e (Cortijo *et al.*, 1994). As a result, rapid changes occurred in ocean circulation and oceanic heat fluxes in high northern latitudes during the Last Interglacial, and induced marked temperature changes on adjacent continents (Fronval and Jansen, 1996). Nevertheless, other records indicate a relatively stable climate during the Last Interglacial. For example, the planktonic foraminiferal assemblages and the abundance of ice-rafted detritus in two North Atlantic marine records (DSDP site 609 and V29-191) showed a stable climate in that region during the Last Interglacial (McManus *et al.*, 1994); and results from benthic foraminifera suggested no changes in North Atlantic Deep Water production during MIS 5e (Keigwin *et al.*, 1994). As such, it implies a different origin of the climate instability observed in Greenland ice cores, challenging the previous consideration of ice flow disturbance. Recently, the hypothesis of climate instability during MIS 5e has been revisited with new high-resolution records. These records indicate a larger amplitude of variability within MIS 5e compared with the Holocene (Tzedakis *et al.*, 2018, and references therein), indicating an unstable Last Interglacial climate in the North Atlantic and Europe.

In China, loess deposits have been used to study the climate during the Last Interglacial, and inconsistent conclusions have been attained in different studies. Fang *et al.*, (1996; 1998) revealed the existence of three periods of strongly enhanced summer monsoon, and two periods of intensified winter monsoon during the Last Interglacial, based on the high deposition rate in loess sequences in the Lanzhou and Linxia areas (western CLP), suggesting unstable climate conditions during MIS 5e. Soon afterwards, An and Porter (1997) identified two dust-flux events when winter monsoon winds strengthened during MIS 5e, identified in multiple loess profiles on the central CLP, using proxies of >40-μm quartz fraction and bulk sediment samples, which are comparable to the stadial events during the last glaciation. These events were also spotted as sand dune formations in the deposits of the Salawusu Group in northern China (Lv *et al.*, 2004). Nevertheless, some other loess studies have suggested that the climate during the Last Interglacial was stable (Liu *et al.*, 1998; Chen *et al.*, 1999; Ding *et al.*, 1999; Guo *et al.*, 1999; Wu *et al.*, 2002; Chen *et al.*, 2003; Guan *et al.*, 2007), even in studies reporting high deposition rates (Chen *et al.*, 2003; Guan *et al.*, 2007). In the case of speleothems, the records from Dongge and Sanbao cave show some changes during the Last Interglacial, but of small amplitude (~0.5–0.8‰, Yuan *et al.*, 2004; Kelly *et al.*, 2006; Wang *et al.*, 2008); while the records from Tianmen cave (south central Tibetan Plateau) and Shangxiaofeng Cave (Shandong Province, China) indicate substantial changes during the periods of overlap (Cai *et al.*, 2010; Xue *et al.*, 2019).

A notable feature of the Xiaotian record is the large amplitude oscillations seen in the $\delta^{18}O$ values (up to 3‰) on millennial to centennial timescales within MIS 5e. As shown in Figure 6, three prominent events occurred at ~128.7–128.3, ~127.3–127.1 and ~126.6–126.4 kyr BP, respectively. The oldest event coincides with the Younger Dryas (YD)-like event identified in the speleothem $\delta^{18}O$ record from Shandong Province, northeastern China (Xue *et al.*, 2019). The two later events could align with the weak monsoon events apparent in the speleothem $\delta^{18}O$ records from Dongge Cave (Kelly *et al.*, 2006) within quoted dating uncertainties. In addition to these three centennial events, three short-duration but larger amplitude oscillations of low $\delta^{18}O$ are apparent during the period 130.1–128.9 kyr BP. Such an increased amplitude indicates enhanced variability of the EASM during the early part of the Last Interglacial and/or penultimate deglaciation, implying possible impacts of the remanent Greenland ice sheet melting at that time. These fluctuations are comparable to the variations registered in the speleothem $\delta^{18}O$ record from Shandong Province (northern China). Similar fluctuations were also found in the $\delta^{18}O$ record from Tianmen Cave, south central Tibetan, another region sensitive to ISM changes (Cai *et al.*, 2010a). All these similarities indicate that there were significant changes occurred in circulation of the ASM and confirm the instability of ASM climate during the Last Interglacial.

Marine proxies from drilling site 980 (North Atlantic) indicate that brief increases in ice-rafted debris and cooling of SST also occurred throughout MIS 5e (Oppo *et al.* 2006), demonstrating the variability of North Atlantic climate during the Last Interglacial. It may imply that variations in the ASM were potentially associated

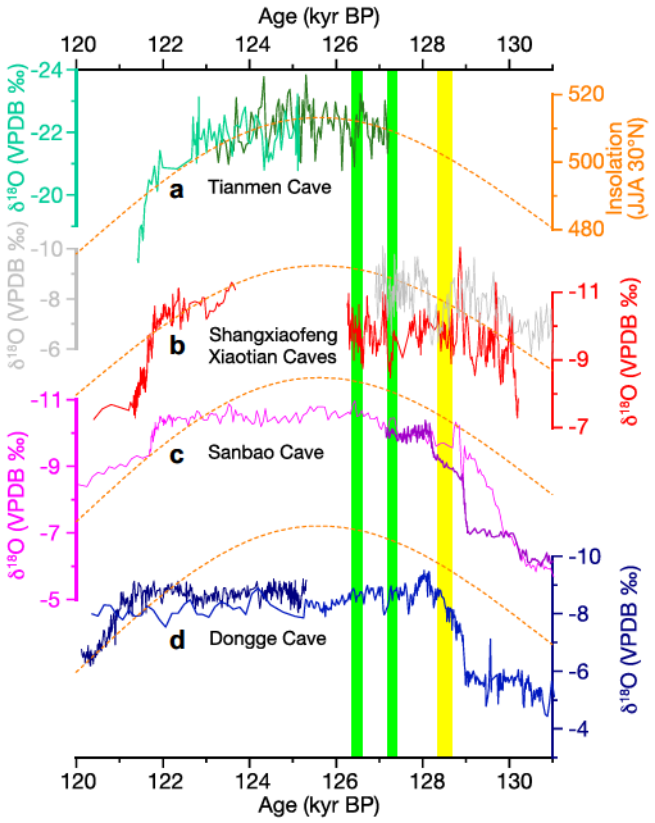

Figure 6. Comparison of oxygen isotopic records from Xiaotian Cave (b, red line, stalagmite XT-4) and Shangxiaofeng Cave (b, grey line, Xue *et al.*, 2019) with $\delta^{18}O$ records from Tianmen Cave (a, Cai *et al.*, 2010), Sanbao (c, Wang *et al.*, 2008) and Dongge Cave (d, Kelly *et al.*, 2006) during Marine Isotope Stage 5e. The dashed orange lines show the Northern Hemisphere summer (JJA) insolation at 30°N. [Color figure can be viewed at wileyonlinelibrary.com]

with climate changes in North Atlantic region (An and Porter, 1997). At face value, it is apparent that for the abrupt events in MIS 5e, all the speleothem $\delta^{18}O$ records from caves in the marginal zone of the Asian monsoon show high $\delta^{18}O$ amplitude (e.g. >2‰ in Tianmen, Shangxiaofeng and Xiaotian caves), while other $\delta^{18}O$ records from southern China indicate relatively reduced amplitude (e.g. <1 ‰ in Dongge and Sanbao caves). This observation probably suggests the heightened sensitivity of precipitation $\delta^{18}O$ to climate changes at the marginal zone of the ASM during the warm and humid interglacial period. An explanation may be that increased humidity, ameliorated hydrological conditions and flourishing vegetation during the Last Interglacial might have buffered the influence of EASM changes on the precipitation $\delta^{18}O$ in southern China through modulation of moisture recycling to some extent, whereas the impacts caused by the evaporation of raindrop beneath the cloud cover in the semi-humid/semi-arid region might be intensified.

Taking all these studies together, it is apparent that significant climate oscillations occurred at high latitudes around the North Atlantic during the Last Interglacial. Conversely, small fluctuations are recorded in pollen records, possibly due to the slow response to the climate of such proxy and diachronous characteristics. Similarly, in Chinese Loess records, only sensitive proxies show variations, whereas the fluctuations on centennial timescales are insignificant in the context of a low sedimentation rate. Although the amplitudes of speleothem $\delta^{18}O$ in southern China are relatively small during the Last Interglacial, these amplitudes are the same as those recorded during the Holocene, indicating a comparable climate instability. It is of note that the amplitude seen during the Last Interglacial, as well as during the Holocene, is relatively smaller than that during the glacial period. Such a difference probably indicates that the climate was relatively stable during the interglacial (warm period) compared with during the glacial (cold period) on millennial to centennial timescales, whereas quite different boundary conditions between glacial and interglacial periods might undermine any direct comparison.

Conclusions

The speleothem $\delta^{18}O$ records from northern China are pivotal to understanding the disparity observed between loess records, largely dominated by the 100-kyr periodicity, and speleothem $\delta^{18}O$ records that show prominent precessional cycles. The isotope records of two stalagmites from Xiaotian Cave, southeast CLP, were used to understand the EASM variations in northern China and associated precipitation $\delta^{18}O$ changes during much of MIS 5 to MIS 3. This record, characterized by prominent precessional variations and punctuated by millennial-scale oscillations and consistent with other Chinese speleothem $\delta^{18}O$ records, suggests that proxies from loess records (e.g. magnetic susceptibility) and speleothem $\delta^{18}O$ records may record different aspects of EASM changes, and so their signals are not synchronous and correlated.

In this record, the $\delta^{18}O$ values during MIS 5e were in the same range as that during MIS 5c and 5a, comparable to other speleothem $\delta^{18}O$ records from EASM regions. This muted response of speleothem $\delta^{18}O$ to the NHSI during MIS 5e probably reflects an equivalent or even increased contribution of moisture from the South China Sea and North Pacific, which is enriched in ^{18}O as compared with moisture from the Indian Ocean and Bay of Bengal, and suggesting that an El Niño-like state existed.

The Xiaotian speleothem $\delta^{18}O$ values increased abruptly at 121.7 kyr BP, consistent with previously reported Chinese speleothem $\delta^{18}O$ records, indicating a regime shift in atmospheric circulation in the Asian monsoon domain. Abrupt changes in sea ice extent or shifts in the mean climate state in the North Atlantic responding to gradually weaking of the NHSI might potentially trigger the abrupt changes in precipitation $\delta^{18}O$ in Asian monsoon regions by affecting the circulation of the westerlies and/or the ITCZ. However, it is not implausible that the decreases in SST of the tropical Indian and Pacific Ocean caused by the decline in insolation reached a certain threshold, resulting in a regime shift in precipitation $\delta^{18}O$, either through weakened convective atmospheric activity over the tropical ocean or through abrupt changes in moisture transport and cycling of tropical moisture sources of the ASM.

Furthermore, centennial-scale changes with large amplitude of up to ~3‰ in speleothem records during the Last Interglacial suggest heightened sensitivity of precipitation $\delta^{18}O$ to climate changes in the marginal zone of the ASM, in a context of warm and humid climate conditions. Taking various studies into consideration, the climatic oscillations during MIS 5e were comparable to that during the Holocene, indicating rather unstable climate conditions during the Last Interglacial.

Acknowledgments. This work was supported by the Strategic Priority Research Program of the Chinese Academy of Sciences (Grant No. XDB 40010200), National Natural Science Foundation of China grants (42130503, 41888101), National Science Foundation of United States (2202913 to RLE), and the Young Talent Support Plan of Xi'an Jiaotong University.

Supporting information

Additional supporting information can be found in the online version of this article.

References

An Z, Porter SC. 1997. Millennial-scale climatic oscillations during the last interglaciation in central China. *Geology* **25**: 603.

An Z, Wu X, Wang P, Wang S, Dong G, Sun X, Zhang D, Lu Y, Zheng S, Zhao S. 1991. Paleomonsoons of China over the last 130000 years. *Science in China Series D-Earth Sciences* **34**: 1007–1024.

Battisti D, Ding Q, Roe G. 2014. Coherent pan-Asian climatic and isotopic response to orbital forcing of tropical insolation. *Journal of Geophysical Research: Atmospheres*:**119**:11997-12020.

Beck JW, Zhou W, Li C, Wu Z, White L, Xian F, Kong X, An Z. 2018. A 550,000-year record of East Asian monsoon rainfall from 10Be in loess. *Science* **360**: 877–881.

Breitenbach SFM, Rehfeld K, Goswami B, Baldini JUL. 2012. COnstructing Proxy Records from Age models (COPRA). *Climate of the Past* **8**: 1765–1779.

Cai Y, An Z, Cheng H, Edwards RL, Kelly MJ, Liu W, Wang X, Shen C-C. 2006. High-resolution absolute-dated Indian Monsoon record between 53 and 36 ka from Xiaobailong Cave, southwest China. *Geology* **34**: 621–624.

Cai Y, Cheng X, Ma L, Mao R, Breitenbach SFM, Zhang H, Xue G, Cheng H, Edwards RL, An Z. 2021. Holocene variability of East Asian summer monsoon as viewed from the speleothem $\delta^{18}O$ records in central China. *Earth and Planetary Science Letters* **558**: 116758.

Cai Y, Fung IY, Edwards RL, An Z, Cheng H, Lee J-E, Tan L, Shen C-C, Wang X, Day JA. 2015. Variability of stalagmite-inferred Indian monsoon precipitation over the past 252,000 y. Proceedings of the National Academy of Sciences 112, 2954-2959.

Cai Y, Zhang H, Cheng H, An Z, Lawrence Edwards R, Wang X, Tan L, Liang F, Wang J, Kelly M. 2012. The Holocene Indian monsoon variability over the southern Tibetan Plateau and its teleconnections. *Earth and Planetary Science Letters* **335–336**: 135–144.

Cai Y, Zhang M, Peng Z, Lin Y, An Z, Zhang Z, Cao Y. 2001. The $\delta^{18}O$ variation of a stalagmite from Qixing Cave, Guizhou Province and indicated climate change during the Holocene. *Chinese Science Bulletin* **46**(22): 1904–1908.

Cai YJ, Cheng H, An ZS, Edwards RL, Wang XF, Tan LC, Wang J. 2010a. Large variations of oxygen isotopes in precipitation over south-central Tibet during Marine Isotope Stage 5. *Geology* **38**: 243–246.

Cai Y, Tan L, Cheng H, An Z, Edwards RL, Kelly MJ, Kong X, Wang X, 2010b. The variation of summer monsoon precipitation in central China since the last deglaciation. *Earth and Planetary Science Letters* **291**, 21-31.

Chappellaz J, Brook E, Blunier T, Malaizé B. 1997. CH_4 and ^{18}O of O_2 records from Antarctic and Greenland ice: A clue for stratigraphic disturbance in the bottom part of the Greenland Ice Core Project and Greenland Ice Sheet Project 2 ice cores. *Journal of Geophysical Research Atmospheres* **102**: 26547–26558.

Chen FH, Bloemendal J, Feng ZD, Wang JM, Parker E, Guo ZT. 1999b. East Asian monsoon variations during Oxygen Isotope Stage 5: evidence from the northwestern margin of the Chinese loess plateau. *Quaternary Science Reviews* **18**: 1127–1135.

Chen FH, Qiang MR, Zeng ZD, Wang HB, Bloemendal J. 2003. Stable East Asian monsoon climate during the Last Interglacial (Eemian) indicated by paleosol S1 in the western part of the Chinese Loess Plateau. *Global and Planetary Change* **36**: 171–179.

Chen J, An Z, Head J. 1999a. Variation of Rb/Sr Ratios in the Loess-Paleosol Sequences of Central China during the Last 130,000 Years and Their Implications for Monsoon Paleoclimatology. *Quaternary Research* **51**: 215–219.

Chen S, Wang Y, Cheng H, Edwards RL, Wang X, Kong X, Liu D. 2016. Strong coupling of Asian Monsoon and Antarctic climates on sub-orbital timescales. *Scientific Reports* **6**: 32995.

Cheng H, Edwards RL, Broecker WS, Denton GH, Kong X, Wang Y, Zhang R, Wang X. 2009. Ice Age Terminations. *Science* **326**: 248–252.

Cheng H, Edwards RL, Sinha A, Spötl C, Yi L, Chen S, Kelly M, Kathayat G, Wang X, Li X. 2016. The Asian monsoon over the past 640,000 years and ice age terminations. *Nature* **534**: 640.

Cheng H, Edwards Lawrence, Shen R, Polyak C-C, Asmerom VJ, Woodhead Y, Hellstrom J, Wang J, Kong Y, Spötl X, Wang C, Calvin X, Alexander E Jr.. 2013. mprovements in ^{230}Th dating, ^{230}Th and ^{234}U half-life values, and U–Th isotopic measurements by multi-collector inductively coupled plasma mass spectrometry. *Earth and Planetary Science Letters* **371–372**: 82–91.

Cheng H, Sinha A, Wang X, Cruz FW, Edwards RL. 2012. The Global Paleomonsoon as seen through speleothem records from Asia and the Americas. *Climate Dynamics* **39**: 1045–1062.

Cheng H, Springer GS, Sinha A, Hardt BF, Yi L, Li H, Tian Y, Li X, Rowe HD, Kathayat G, Ning Y, Edwards RL. 2019. Eastern North American climate in phase with fall insolation throughout the last three glacial-interglacial cycles. *Earth and Planetary Science Letters* **522**: 125–134.

Cheng H, Zhang H, Cai Y, Shi Z, Yi L, Deng C, Hao Q, Peng Y, Sinha A, Li H, Zhao J, Tian Y, Baker J, Perez-Mejías C. 2021. Orbital-scale Asian summer monsoon variations: Paradox and exploration. *Science China Earth Sciences* **64**: 529–544.

Cheng H, Xu Y, Dong X, Zhao J, Li H, Baker J, Sinha A, Spötl C, Zhang H, Du W. 2021. Onset and termination of Heinrich Stadial 4 and the underlying climate dynamics. *Communications Earth & Environment* **2**: 1–11.

Chiang JCH, Fung IY, Wu C-H, Cai Y, Edman JP, Liu Y, Day JA, Bhattacharya T, Mondal Y, Labrousse CA. 2015. Role of seasonal transitions and westerly jets in East Asian paleoclimate. *Quaternary Science Reviews* **108**: 111–129.

Cortijo E, Duplessy JC, Labeyrie L, Leclaire H, Duprat J, van Wearing TCE. 1994. Eemian cooling in the Norwegian Sea and North Atlantic Ocean preceding continental ice-sheet growth. *Nature* **372**: 446–449.

Dansgaard W, Johnsent SJ, Clausen HB, Dahl-Jensen D, Gundestrup NS, Hammer CU, Hvidberg CS, Steffensen JP, Sveinbjornsdottir AE, Jouzel J, Bond G. 1993. Evidence for general instability of past climate from a 250-kyr ice-core record. *Nature* **364**: 218–220.

Ding Y-H, Chan JCL. 2005. The East Asian summer monsoon: an overview. *Meteorology and Atmospheric Physics* **89**: 117–142.

Ding Y, Wang Z, Sun Y. 2007. Interdecadal variation of the summer precipitation in East China and its association with decreasing Asian monsoon. Part I: observed evidences. *Int. J. Climatol.* **28**: 1139–1161.

Ding ZL, Ren JZ, Yang SL, Liu TS. 1999. Climate instability during the penultimate glaciation: Evidence from two high-resolution loess records, China. *Journal of Geophysical Research* **104**: 20.

Dorale JA, Edwards RL, Ito E, Gonza«lez LA. 1998. Climate and Vegetation History of the Midcontinent from 75 to 25 ka: A Speleothem Record from Crevice Cave, Missouri, USA. *Science* **282**: 1871–1874.

Edwards RL, Chen JH, Wasserburg GJ. 1987. ^{238}U-^{234}U-^{230}Th-^{232}Th systematic and the precise measurement of time over the past 500,000 years. *Earth and Planetary Science Letters* **81**: 175–192.

Fang XM, Dai XR, Li JJ, Cao JX, Guan DH, Hao YP, Wang JL, Wang JM. 1996. The abruptness and instability of Asian monsoon evolution as observed from the last interglacial palaeosoil. *Science in China, series D.* **26**(002): 154–160. https://doi.org/10.1360/zd1996-26-2-154 (in Chinese)

Fang XM, Li JJ, Banerjee S, Dai XR, Guan DH. 1998. The study on environmental rock magnetism of abrupt summer monsoon changes during the last interglacial MIS5e substage. *Chinese Science Bulletin, 1998* **43**(021): 2330–2332. https://doi.org/10.1360/csb1998-43-21-2330 (in Chinese)

Feng ZD, Wang HB, Olson CG. 2004. Pedogenic factors affecting magnetic susceptibility of the last interglacial paleosol S1 in the Chinese Loess Plateau. *Earth Surface Processes and Landforms* **29**: 1384–1402. https://doi.org/10.1002/esp.1110

Fohlmeister J, Ny Riavo GV, Lechleitner FA, Boyd M, Brandtstätter S, Jacobson MJ, Oster J. 2020. Main Controls on the Stable Carbon Isotope Composition of Speleothems. *Geochimica et Cosmochimica Acta* **279**: 67-87. https://doi.org/10.1016/j.gca.2020.03.042

Fronval T, Jansen E. 1996. Rapid changes in ocean circulation and heat flux in the Nordic seas during the last interglacial period. *Nature* **383**: 806–810.

Fuchs A, Leuenberger MC. 1996. $\delta^{18}O$ of atmospheric oxygen measured on the GRIP ice core document stratigraphic disturbances in the lowest 10% of the core. *Geophysical Research Letters* **23**: 1049–1052.

Genty D, Blamart D, Ghaleb B, Plagnes V, Causse C, Bakalowicz M, Zouari K, Chkir N, Hellstrom J, Wainer K, Bourges F. 2006. Timing

and dynamics of the last deglaciation from European and North African delta C-13 stalagmite profiles - comparison with Chinese and South Hemisphere stalagmites. *Quaternary Science Reviews* **25**: 2118–2142.

Greenland Ice-core Project, M. 1993. Climate instability during the last interglacial period recorded in the GRIP ice core. *Nature* **364**: 203–207.

Grootes PM, Stulver M, White JWC, Johnson S, Jouzel J. 1993. Comparison of Oxygen isotope records from the GISP2 and GRIP Greenland ice cores. *Nature* **366**: 552–554.

Guan QY, Pan BT, Gao HS, Li BY, Wang JP, Su H. 2007. The instability of East Asian monsoon during the last interglacial recorded by high-resolution loess profile. *Science China, series D.* **37**(1): 86–93. https://doi.org/10.3969/j.issn.1674-7240.2007.01.010 (in Chinese)

Guo ZT, Peng SZ, Wei LY, Liu TS. 1999, Millennial-scale oscillations of the East Asian summer monsoon over the last 0.220 Ma, Quaternary Sciences, 1999, 4:299-305, https://doi.org/10.1088/0256-307X/15/11/025 (in Chinese with English abstract).

Held IM, Soden BJ. 2006. Robust responses of the hydrological cycle to global warming. *Journal of Climate* **19**: 5686–5699.

Hendy CH. 1971. The isotopic geochemistry of speleothems--I. The calculation of the effects of different modes of formation on the isotopic composition of speleothems and their applicability as palaeoclimatic indicators. *Geochim Cosmochim Ac* **35**: 801–824.

Johnsen SJ, Clausen HB, Dansgaard W, Gundestrup NS, Hammer CU, Tauber H. 1995. The Eem Stable Isotope Record along the GRIP Ice Core and Its Interpretation. *Quaternary Research* **43**: 117–124.

Johnsen SJ, Clausen HB, Dansgaard W, Gundestrup NS, Hammer CU, Andersen U, Andersen KK, Hvidberg CS, Dahl-Jensen D, Steffensen JP, Shoji H, Sveinbjörnsdóttir ÁE, White J, Jouzel J, Fisher D. 1997. The $\delta^{18}O$ record along the Greenland Ice Core Project deep ice core and the problem of possible Eemian climatic instability. *Journal of Geophysical Research: Oceans* **102**: 26397–26410.

Johnson KR, Ingram BL. 2004. Spatial and temporal variability in the stable isotope systematics of modern precipitation in China: implications for paleoclimate reconstructions. *Earth and Planetary Science Letters* **220**: 365–377.

Kathayat G, Cheng H, Sinha A, Spötl C, Edwards RL, Zhang H, Li X, Yi L, Ning Y, Cai Y, Lui WL, Breitenbach SFM. 2016. Indian monsoon variability on millennial-orbital timescales. *Scientific Reports* **6**: 24374.

Keigwin LD, Curry WB, Lehman SJ, Johnsen S. 1994. The role of the deep ocean in North Atlantic climate change between 70 and 130 kyr ago. *Nature* **371**: 323–326.

Kelly MJ, Edwards RL, Cheng H, Yuan DX, Cai YJ, Zhang ML, Lin YS, An ZS. 2006. High resolution characterization of the Asian Monsoon between 146,000 and 99,000 years BP from Dongge Cave, China and global correlation of events surrounding Termination II. *Palaeogeography Palaeoclimatology Palaeoecology* **236**: 20–38.

Kim S-T, O'Neil JR. 1997. Equilibrium and nonequilibrium oxygen isotope effects in synthetic carbonates. *Geochim Cosmochim Ac* **61**: 3461–3475.

Kukla GJ. 2000. The last interglacial. *Science* **287**: 987–988.

Kukla GJ, Bender ML, de Beaulieu J-L, Bond G, Broecker WS, Cleveringa P, Gavin JE, Herbert TD, Imbrie J, Jouzel J. 2002. Last Interglacial Climates. *Quaternary Research* **58**: 2–13.

Kutzbach JE. 1981. Monsoon climate of the Early Holocene: Climate experiment with the Earth's orbital parameters for 9000 years ago. *Science* **214**: 59–61.

Kutzbach J, Liu X, Liu Z, Chen G. 2008. Simulation of the evolutionary response of global summer monsoons to orbital forcing over the past 280,000 years. *Climate Dynamics* **30**: 567–579.

Lechleitner FA, Breitenbach SFM, Cheng H, Plessen B, Rehfeld K, Goswami B, Marwan N, Eroglu D, Adkins JF, Haug GH. 2017. Climatic and in-cave influences on $\delta^{18}O$ and $\delta^{13}C$ in a stalagmite from northeastern India through the last deglaciation. *Quaternary Research* **88**: 458–471. https://doi.org/10.1017/qua.2017.72

Lee J-E, Risi C, Fung I, Worden J, Scheepmaker RA, Lintner B, Frankenberg C. 2012. Asian monsoon hydrometeorology from TES and SCIAMACHY water vapor isotope measurements and LMDZ simulations: Implications for speleothem climate record interpretation. *Journal of Geophysical Research: Atmospheres* **117**: D15112. https://doi.org/10.1029/2011JD017133

Levermann A, Schewe J, Petoukhov V, Held H. 2009. Basic mechanism for abrupt monsoon transitions. Proceedings of the National Academy of Sciences 106, 20572.

Li T, Liu F, Abels HA, You C-F, Zhang Z, Chen J, Ji J, Li L, Li L, Liu H-C, Ren C, Xia R, Zhao L, Zhang W, Li G. 2017. Continued obliquity pacing of East Asian summer precipitation after the mid-Pleistocene transition. *Earth and Planetary Science Letters* **457**: 181–190.

Li Y, Rao Z, Xu Q, Zhang S, Liu X, Wang Z, Cheng H, Edwards RL, Chen F. 2020. Inter-relationship and environmental significance of stalagmite $\delta^{13}C$ and $\delta^{18}O$ records from Zhenzhu Cave, north China, over the last 130 ka. *Earth and Planetary Science Letters* **536**: 116149.

Liu XM, Hesse P, Liu TS, Bloemendal J. 1998. High resolution climate record from the Beijing area during the last glacial-interglacial cycle. *Geophysical Research Letters* **25**(3): 349–352.

Liu X, Liu J, Chen S, Chen J, Zhang X, Yan J, Chen F. 2020b. New insights on Chinese cave $\delta^{18}O$ records and their paleoclimatic significance. *Earth-Science Reviews* **207**: 103216.

Liu G, Li X, Chiang H-W, Cheng H, Yuan S, Chawchai S, He S, Lu Y, Aung L, Maung P. 2020a. On the glacial-interglacial variability of the Asian monsoon in speleothem $\delta^{18}O$ records. *Science advances* **6**: eaay8189.

Liu TH, Chang FN, Li TG, Sun HJ, Cui YK, Wang J, Qian F. 2020c. ENSO-like state in the tropical Pacific Ocean during the cold and warm periods of the glacial cycle since 450 ka. Quaternary. *Sciences* **40**(3): 646–657 (in Chinese with English abstract).

Liu Z, Wen X, Brady E, Otto-Bliesner B, Yu G, Lu H, Cheng H, Wang Y, Zheng W, Ding Y. 2014. Chinese cave records and the East Asia summer monsoon. *Quaternary Science Reviews* **83**: 115–128.

Lv HY, Han JM, Wu NQ, Guo ZT. 1994. Analysis on magnetism and paleoclimate meaning in modern soil of China. *Science in China (series B)* **24**(12): 1290–1297 (in Chinese).

Lv YX, Li BS, Jin HL, Zhang DD, Yu XF. 2004. Major Element Record in Salawusu River Valley Responding to Global Change during Last Interglacial Period. *Journal of Desert Research* **24**(2): 136–143. https://doi.org/10.3321/j.issn:1000-694X.2004.02.004 (in Chinese with English abstract)

Ma L, Li Y, Liu X, Sun Y. 2017. Registration of precession signal in the Last Interglacial paleosol (S1) on the Chinese Loess Plateau. *Geochemistry, Geophysics, Geosystems* **18**: 3964–3975.

Maher BA. 2008. Holocene variability of the East Asian summer monsoon from Chinese cave records: a re-assessment. *Holocene* **18**: 861–866.

McDermott F. 2004. Palaeo-climate reconstruction from stable isotope variations in speleothems: a review. *Quaternary Science Reviews* **23**: 901–918.

McManus JF, Bond GC, Broecker WS, Johnsen S, Labeyrie L, Higgins S. 1994. High-resolution climate records from the North Atlantic during the last interglacial. *Nature* **371**: 326–329.

North-Greenland-Ice-Core-Project-members. 2004. High-resolution record of Northern Hemisphere climate extending into the last interglacial period. *Nature* **431**: 147–151.

Oppo DW, McManus JF, Cullen JL. 2006. Evolution and demise of the Last Interglacial warmth in the subpolar North Atlantic. *Quaternary Science Reviews* **25**: 3268–3277.

Pausata FSR, Battisti DS, Nisancioglu KH, Bitz CM. 2011. Chinese stalagmite $\delta^{18}O$ controlled by changes in the Indian monsoon during a simulated Heinrich event. *Nat Geosci* **4**: 474–480.

Pérez-Mejías C, Moreno A, Sancho C, Bartolomé M, Stoll H, Osácar MC, Cacho I, Delgado-Huertas A. 2018. Transference of isotopic signal from rainfall to dripwaters and farmed calcite in Mediterranean semi-arid karst. *Geochimica et Cosmochimica Acta* **243**: 66–98.

Pérez-Mejías C, Moreno A, Sancho C, Martín-García R, Spötl C, Cacho I, Cheng H, Edwards RL. 2019. Orbital-to-millennial scale climate variability during Marine Isotope Stages 5 to 3 in northeast Iberia. *Quaternary Science Reviews* **224**: 105946.

Porter SC, An ZS. 1995. Correlation between climate events in the North Atlantic and China during the last glaciation. *Nature* **375**: 185–188.

Rao ZG, Liu XK, Hua H, Gao YL, Chen FH. 2015. Evolving history of the East Asian summer monsoon intensity during the MIS5: inconsistent records from Chinese stalagmites and loess deposits. *Environmental Earth Sciences* **73**(7): 3937–3950.

Ridley HE, Asmerom Y, Baldini JUL, Breitenbach SFM, Aquino VV, Prufer KM, Culleton BJ, Polyak V, Lechleitner FA, Kennett DJ, Zhang MH, Marwan N, Macpherson CG, Baldini LM, Xiao TY, Peterkin JL, Awe J, Haug GH. 2015. Aerosol forcing of the position of the intertropical convergence zone since AD 1550. *Nature Geoscience* **8**: 195–200.

Rohling EJ, Liu QS, Roberts AP, Stanford JD, Rasmussen SO, Langen PL, Siddall M. 2009. Controls on the East Asian monsoon during the last glacial cycle, based on comparison between Hulu Cave and polar ice-core records. *Quaternary Science Reviews* **28**: 3291–3302.

Schewe J, Levermann A, Cheng H. 2012. A critical humidity threshold for monsoon transitions. *Climate of the Past*. **8**:535-544.

Shi Z, Cai Y, Liu X, Sha Y. 2018. Distinct responses of East Asian and Indian summer monsoons to astronomical insolation during Marine Isotope Stages 5c and 5e. *Palaeogeography, Palaeoclimatology, Palaeoecology* **510**: 40–48.

Shi ZG, Liu XD, Sun YB, An ZS, Liu Z, Kutzbach J. 2011. Distinct responses of East Asian summer and winter monsoons to astronomical forcing. *Climate of the Past* **7**(4): 1363–1370.

Spratt RM, Lisiecki LE. 2016. A Late Pleistocene sea level stack. *Climate of the Past* **12**: 1079–1092.

Sun Y, Clemens SC, An Z, Yu Z. 2006. Astronomical timescale and palaeoclimatic implication of stacked 3.6-Myr monsoon records from the Chinese Loess Plateau. *Quaternary Science Reviews* **25**: 33–48.

Sun Y, Kutzbach J, An Z, Clemens S, Liu Z, Liu W, Liu X, Shi Z, Zheng W, Liang L, Yan Y, Li Y. 2015. Astronomical and glacial forcing of East Asian summer monsoon variability. *Quaternary Science Reviews* **115**: 132–142.

Sun Y, Yin Q, Crucifix M, Clemens SC, Araya-Melo P, Liu W, Qiang X, Liu Q, Zhao H, Liang L, Chen H, Li Y, Zhang L, Dong G, Li M, Zhou W, Berger A, An Z. 2019. Diverse manifestations of the mid-Pleistocene climate transition. *Nature Communications* **10**: 352.

Tan M. 2014. Circulation effect: response of precipitation $\delta^{18}O$ to the ENSO cycle in monsoon regions of China. *Climate Dynamics* **42**: 1067–1077.

Taylor K, Hammer C, Alley RB, Clausen H, Dahl-Jensen D, Gow A, Gundestrup N, Kipfstuh J, Moore J, Waddington E. 1993. Electrical conductivity measurements from the GISP2 and GRIP Greenland ice cores. *Nature* **366**: 549–552.

Tzedakis PC, Drysdale RN, Margari V, Skinner LC, Menviel L, Rhodes RH, Taschetto AS, Hodell DA, Crowhurst SJ, Hellstrom JC, Fallick AE, Grimalt JO, McManus JF, Martrat B, Mokeddem Z, Parrenin F, Regattieri E, Roe K, Zanchetta G. 2018. Enhanced climate instability in the North Atlantic and southern Europe during the Last Interglacial. *Nature Communications* **9**: 4235. https://doi.org/10.1038/S41467-018-06683-3

Vecchi GA, Soden BJ, Wittenberg AT, Held IM, Leetmaa A, Harrison MJ. 2006. Weakening of tropical Pacific atmospheric circulation due to anthropogenic forcing. *Nature* **441**: 73–76.

Wang B, Wu R, Fu X. 2000. Pacific–East Asian teleconnection: how does ENSO affect East Asian climate? *Journal of Climate* **13**: 1517–1536.

Wang Y, Cheng H, Edwards RL, Kong X, Shao X, Chen S, Wu J, Jiang X, Wang X, An Z. 2008. Millennial- and orbital-scale changes in the East Asian monsoon over the past 224,000 years. *Nature* **451**: 1090–1093.

Wang YJ, Cheng H, Edwards RL, An ZS, Wu JY, Shen C-C, Dorale JA. 2001. A high-resolution absolute-dated late Pleistocene Monsoon record from Hulu cave, China. *Science* **294**: 2345–2348.

Winter A, Zanchettin D, Lachniet M, Vieten R, Pausata FSR, Ljungqvist FC, Cheng H, Edwards RL, Miller T, Rubinetti S, Rubino A, Taricco C. 2020. Initiation of a stable convective hydroclimatic regime in Central America circa 9000 years BP. *Nature Communications* **11**: 716.

Wu GJ, Pan BT, Guan QY, Liu ZG, Li JJ. 2002. Loess record of climatic changes during MIS5 in the Hexi Corridor, northwest China. *Quaternary International* **97**: 167–172.

Wu Y, Li T-Y, Yu T-L, Shen C-C, Chen C-J, Zhang J, Li J-Y, Wang T, Huang R, Xiao S-Y. 2020. Variation of the Asian summer monsoon since the last glacial-interglacial recorded in a stalagmite from southwest China. *Quaternary Science Reviews* **234**: 106261.

Xue G, Cai Y, Lu Y, Ma L, Cheng X, Liu C, Yan H, Sun Y, Li D, Wei Y, Huang S, He M, Cheng H, Edwards RL. 2021. Speleothem-based hydroclimate reconstructions during the penultimate deglaciation in Northern China. Paleoceanography and Paleoclimatology n/a, e2020PA004072.

Xue G, Cai Y, Ma L, Cheng X, Cheng H, Edwards RL, Li D, Tan L. 2019. A new speleothem record of the penultimate deglacial: Insights into spatial variability and centennial-scale instabilities of East Asian monsoon. *Quaternary Science Reviews* **210**: 113–124.

Yin QZ, Wu ZP, Berger A, Goosse H, Hodell D. 2021. Insolation triggered abrupt weakening of Atlantic circulation at the end of interglacials. *Science* **373**: 1035–1040.

Yuan D, Cheng H, Edwards RL, Dykoski CA, Kelly MJ, Zhang M, Qing J, Lin Y, Wang Y, Wu J, Dorale JA, An Z, Cai Y. 2004. Timing, Duration, and Transitions of the Last Interglacial Asian Monsoon. *Science* **304**: 575–578.

Zhang Z, Li G, Cai Y, Liu Z, An Z. 2021. Variation of summer precipitation $\delta^{18}O$ on the Chinese Loess Plateau since the last interglacial. *Journal of Quaternary Science* **36**: 1214-1220. https://doi.org/10.1002/jqs.3358

Ziegler M, Lourens LJ, Tuenter E, Hilgen F, Reichart G-J, Weber N. 2010. Precession phasing offset between Indian summer monsoon and Arabian Sea productivity linked to changes in Atlantic overturning circulation. *Paleoceanography* **25**: PA3213.